NASA CONTRACTOR
REPORT

NASA CR-129039

CHARACTERIZATION OF NICKEL-COPPER ALLOY SPECIMENS PROCESSED AS A PART OF THE M553 SPHERE FORMING EXPERIMENT DURING THE SKYLAB 1 AND 2 FLIGHT

By J. L. Hubbard, J. W. Johnson, and J. L. Brown
Georgia Institute of Technology
Atlanta, Georgia 30332

December 1973

Prepared for

NASA-GEORGE C. MARSHALL SPACE FLIGHT CENTER
Marshall Space Flight Center, Alabama 35812

TECHNICAL REPORT STANDARD TITLE PAGE

1 REPORT NO.	2. GOVERNMENT ACCESSION NO.	3. RECIPIENT'S CATALOG NO.
NASA CR-129039		

4 TITLE AND SUBTITLE	5. REPORT DATE
Characterization of Nickel-Copper Alloy Specimens Processed as a Part of the M553 Sphere Forming Experiment During the Skylab 1/2 Flight	December 1973
	6. PERFORMING ORGANIZATION CODE
7 AUTHOR(S) J. L. Hubbard, J.W. Johnson, J. L. Brown	8. PERFORMING ORGANIZATION REPORT #
9 PERFORMING ORGANIZATION NAME AND ADDRESS Georgia Institute of Technology Atlanta, Georgia 30332	10. WORK UNIT NO.
	11. CONTRACT OR GRANT NO. NAS 8-28735
12 SPONSORING AGENCY NAME AND ADDRESS National Aeronautics and Space Administration Washington, D. C. 20546	13. TYPE OF REPORT & PERIOD COVERED Contractor Report Summary
	14. SPONSORING AGENCY CODE

15 SUPPLEMENTARY NOTES

16. ABSTRACT

Two specimens of a nickel-copper alloy were processed as a part of the M553 Sphere Forming Experiment during the Skylab 1/2 flight. Both of these specimens were apparently completely melted by the electron beam in the Skylab M512 Materials Processing Facility and either floated free in space, but collided with some smooth flat surface before solidifying or remained attached to its support post during solidification. Both specimens had a smooth flat area on the surface due to this adherence during solidification.

The nominal composition of this alloy before processing in space was 70 percent Ni, 30 percent Cu. Tests have shown that a considerable amount of copper was lost during processing by evaporation. It was further found that less copper was present in the cap areas, particularly at the surface, than was in the remainder of the specimens. The microchemistry of the dendrites and interdendritic regions however, is in agreement with the phase diagram for this alloy.

The measured densities of these specimens were less than the theoretical density of this alloy due to the amount of porosity present, however, no large voids were found by radiographic techniques.

17. KEY WORDS	18. DISTRIBUTION STATEMENT
	Unclassified - Unlimited

19 SECURITY CLASSIF. (of this report)	20. SECURITY CLASSIF. (of this page)	21. NO. OF PAGES	22. PRICE
Unclassified	Unclassified	31	NTIS

TABLE OF CONTENTS

SUMMARY 1

CHARACTERIZATION PROCEDURES 2

CHARACTERIZATION RESULTS 6

DISCUSSION OF RESULTS 10

LIST OF ILLUSTRATIONS

Figure	Title	Page
1.	Profile view of Specimen SL-1.8 (10X).	11
2.	Profile view of ground base Specimen 2-10 (10X)	11
3.	Scanning electron micrograph taken normal to flat area on Specimen SL-1.8 (25X)	12
4.	Scanning electron micrograph of columnar dendrites on the surface of Specimen SL-1.8 (25X)	12
5.	Scanning electron micrograph of columnar dendrites on the surface of Specimen SL-1.8 (250X).	13
6.	Scanning electron micrograph showing the three surface textures on Specimen SL-1.8 (25X).	13
7.	Scanning electron micrograph of the abrupt transition from the porous band to the cap area in Specimen SL-1.8 (250X) . . .	14
8.	Scanning electron micrograph of the abrupt transition from the porous band to the cap area in Specimen SL-1.8 (250X) . . .	14
9.	Scanning electron micrograph of the circular dendrites in the cap region of Specimen SL-1.8 (250X).	15
10.	Scanning electron micrograph of the circular dendrites in the cap region of Specimen SL-1.8 (250X).	15
11.	Oblique view of the cap boundary on Specimen SL-1.8 (25X). . .	16
12.	Oblique view of the cap boundary on Specimen SL-1.8 (100X) . .	16
13.	Optical macrograph of the polished and etched cross section of Specimen SL-1.8 (10X)	17

LIST OF ILLUSTRATIONS (Continued)

Figure	Title	Page
14.	Scanning electron micrograph of the cross section of Specimen SL-1.8 near the cap region (100X).	17
15.	Optical micrograph of the cross section of Specimen SL-1.8 near the porous band (100X).	18
16.	Scanning electron micrograph of the cross section of Specimen SL-1.8 near the porous band (100X)	18
17.	Optical micrograph of the cross section of Specimen SL-1.8 in the equiaxed dendritic region (100X).	19
18.	Scanning electron micrograph of the cross section of Specimen SL-1.8 in the equiaxed dendritic region (250X).	19
19.	Optical micrograph of the columnar dendrites in the cross section of Specimen SL-1.8 (100X).	20
20.	Scanning electron micrograph of the columnar dendrites in the cross section of Specimen SL-1.8 (100X)	20
21.	Profile view of Specimen SL-1.7 (10X).	21
22.	Scanning electron micrograph of columnar dendrites on the surface of Specimen SL-1.7 (400X).	21
23.	Scanning electron micrograph of the dendrites in the porous band on Specimen SL-1.7 (750X).	22
24.	Scanning electron micrograph of the edge of the cap region on Specimen SL-1.7 (150X).	22
25.	Scanning electron micrograph of the circular dendrites in the cap region of Specimen SL-1.7 (750X)	23

LIST OF ILLUSTRATIONS (Concluded)

Figure	Title	Page
26.	Scanning electron micrograph of the circular dendrites in the cap region of Specimen SL-1.7 (750X).	23
27.	Copper concentration versus distance from specimen surface in the central dendritic region of Specimen SL-1.7	24
28.	Copper concentration versus distance from specimen surface in the cap region of Specimen SL-1.7.	25
29.	Optical micrograph of the polished and etched cross section of Specimen SL-1.7 at the edge of the cap area (100X).	26

SUMMARY

Two specimens of a nickel-copper alloy were processed as a part of the M553 Sphere Forming Experiment during the Skylab 1/2 flight. Both of these specimens were apparently completely melted by the electron beam in the Skylab M512 Materials Processing Facility and either floated free in space, but collided with some smooth flat surface before solidifying or remained attached to its support post during solidification. Both specimens had a smooth flat area on the surface due to this adherence during solidification.

Solidification began from the flat contact region with the growth of columnar dendrites which extend from the flat region through about one third of the specimen. This columnar dendritic region is followed by a region of randomly oriented equiaxed dendrites. A large amount of porosity is associated with these dendrites on the surface of the specimens due to solidification shrinkage. The portion of the sample surface directly opposite the flat region is covered with a continuous cap made up of fine circular dendrites.

The nominal composition of this alloy before processing in space was 70 percent Ni, 30 percent Cu. Tests have shown that a considerable amount of copper was lost during processing by evaporation. It was further found that less copper was present in the cap areas, particularly at the surface, than was in the remainder of the specimens. The microchemistry of the dendrites and interdendritic regions however, is in agreement with the phase diagram for this alloy.

The measured densities of these specimens were less than the theoretical density of this alloy due to the amount of porosity present, however, no large voids were found by radiographic techniques.

There was some contamination on the surfaces of these specimens. Some of this was attributable to particles from the support posts but the remainder is unexplained.

CHARACTERIZATION PROCEDURES

Visual Observations

Each of the Skylab specimens was carefully observed under a stereo microscope. Precise notes were taken concerning the shape of the specimens, the degree of melting, the presence of surface contaminants, and the position and nature of any unusual features.

Optical Macroscopy

Optical macrographs were taken of each of the specimens from at least four different orthogonal directions. These macrographs were taken on a Bausch & Lomb "L" camera using a 48 millimeter Micro Tessar lens or on a Polaroid MP-3 camera setup. A few stereomacrographs were recorded using a 6 degree tilt between the left and right views.

Radiography

Radiographs of each of the specimens were made using a Baltograph II x-ray generator operating at 135 KV with a tungsten target to reveal the position and size of any voids present.

Sphericity

Sphericity measurements were made using a micrometric technique which is reported in the results as the ratio of the maximum radius to the minimum radius of the specimen.

Density

The density was measured using a buoyancy technique comparing the weight of the specimen in air and in water. Because of the porosity on the surface of the specimen, ultrasonics was used to facilitate complete wetting of the specimen by the water.

Grain Size Measurements

The Laue grain size was measured from a pattern obtained with a Laue pin hole camera back reflection technique. A Picker x-ray generator

using Cu radiation was used to obtain this pattern. Surface grain sizes were measured directly from scanning electron micrographs.

Scanning Electron Microscopy

A Cambridge Stereoscan Mark II-A scanning electron microscope and an AMR 1000 scanning electron microscope, both equipped with energy dispersive x-ray analyzers were used to examine the Skylab specimens. Each of the specimens was mounted in a special stub designed to hold spheres and placed in the scanning electron microscope for observations. Micrographs of the surface were taken using the following systematic technique. Some great circle on the surface of each sample was chosen on which were exemplified all of the different surface features characteristic of that particular specimen. Low magnification micrographs (25X) were made in the scanning electron microscope along that great circle at intervals of 30 degrees. Higher magnification micrographs were made in each area to show the typical surface structures, any unusual features, and any surface contaminants. The location of the area from which the higher magnification micrographs were made was marked on the low magnification shots. A few stereomicrographs were recorded using a 10 degree difference between the left and right views. Energy dispersive x-ray analysis for elemental content was performed on general areas of each specimen as well as along specific features, on unusual features, and on contaminant particles.

Electron Probe Microanalysis

The electron probe microanalyzer was used for a more accurate analysis of the elemental content. Analyses were run in general areas of each specimen as well as on any unusual features found either through the optics of the microprobe or previously in the scanning electron microscope.

X-Ray Fluorescence Spectroscopy

Quantitative elemental analysis of each sample on a gross scale was made using a Siemens Crystalloflex IV x-ray fluorescence unit operating at 40 KV with a tungsten target.

Section Preparations

Each of the specimens was positioned so that a cut could be made through a plane whose perimeter included all of the various structures seen on the specimen surface. Sectioning was done on a Micromatic Precision Wafering Machine using a 10 mil thick silicon carbide wheel or on a diamond

wire saw. After sectioning, one half of each of the specimens was mounted in a casting resin so that the cut face could be prepared for examination. The specimens were mechanically polished using a series of abrasive papers and wet polishing wheels through a 0.3 micron alumina. Specimen SL-1.8 was electropolished using a Disa-Electropolisher. Electropolishing was accomplished using the E2 electrolyte solution containing:

Cupric nitrate	0.5 kg
Concentrated HNO_3	30×10^{-6} m^3
Methyl alcohol	900×10^{-6} m^3

The sections were etched after electron microprobe analysis was performed. Specimen SL-1.8 was etched with Carapella's reagent containing:

Ferric chloride	5×10^{-3}kg
Concentrated HCL	2×10^{-6} m^3
Methyl alcohol	99×10^{-6} m^3

Specimen SL-1.7 was etched using:

Concentrated HNO_3	50 percent
Glacial Acetic Acid	50 percent

Lattice Parameter and Curie Point Measurements

The lattice parameter was measured using an x-ray diffractometer technique on the section of the specimen. The Curie Point was measured using a DuPont 900 differential scanning calorimeter.

Emission Spectroscopy

A small amount of material was removed from the center of the unmounted half of each specimen by drilling a small shallow hole in the center of each cut face. The shavings thus produced were placed in a cavity of a carbon spectrographic rod and burned to completion in an Applied Research Laboratories 1.5 meter grating emission spectrograph. The near ultraviolet radiation was recorded on Kodak Spectrum Analysis No. 1 Film and analyzed on an Applied Research Laboratories comparator.

Electron Probe Microanalysis of Sections

Each of the polished sections was analyzed in the electron microprobe. Analyses were made of general areas of the sections, across grains, in and along dendritic features, in eutectics and in any unusual features seen. Standards supplied by Dr. Theo Kattamis of the University of Connecticut were used to obtain quantitative data from these analyses.

Optical Examination of Specimen Sections

Optical macrographs of each of the polished and etched sections were taken using a Bausch and Lomb "L" camera and a 48 millimeter lens or a Polaroid MP-3 camera setup, Micrographs were taken to demonstrate all of the various microstructures present on each section using a Leitz Metallux or a Reichert Metallograph optical microscope.

Scanning Electron Microscopy of Sections

Each of the specimen sections was removed from its mount and placed in the scanning electron microscope for observation. Micrographs were taken of both typical and unusual features and some nondispersive x-ray analyses were performed.

CHARACTERIZATION RESULTS

Specimen SL-1.8

Specimen SL-1.8 is a nickel-copper alloy which is nearly spherical in shape except for a very flat smooth region on which the specimen sat during solidification. Figure 1 is a profile view of this specimen showing the flat contact region on the right. From the flat region to almost half way up the specimen, the surface is a smooth tight structure of columnar dendrites. Above this region there is a band in which the structure becomes increasingly rougher and more porous until it ends abruptly in a smooth nonporous cap which covers the top one-third or more of the specimen. This cap appears to be made up of small circular dendrites. The surface structure of this specimen is very similar to that of the nickel-copper ground base Specimen 2-10, as shown in Figure 2.

A gold stain was observed on one side of the specimen.

Radiography revealed no large voids present in the specimen.

Figure 3 is a low power scanning electron micrograph taken normal to the flat region of Specimen SL-1.8. The columnar dendritic structure is seen radiating from this flat area in the top portion of this micrograph. Figure 4 is a micrograph taken 90° away from Figure 3 and shows the flat region at the top, the columnar dendritic region in the center, and the beginning of the more porous band at the bottom. A higher magnification micrograph of the smooth columnar dendritic structure is shown in Figure 5. Figure 6 shows the three different surface structures on the specimen. The abrupt end of the porous band and the beginning of the cap are shown in Figures 7 and 8. The small circular dendrites which make up the cap are shown in Figures 9 and 10. Figure 9 was taken normal to this surface. Figure 10 was taken at an oblique angle to demonstrate the relief of these dendrites. An oblique view of the cap boundary is shown in Figures 11 and 12. Figure 12 shows the large amount of porosity which is present beneath the cap surface.

The surface of the sample contained a large number of contaminating particles. The following elements were found in varying amounts on those

particles analyzed using energy dispersive x-ray analysis:

Al, Si, S, Cl, K, Ca, Ag and Ti

A number of Al_2O_3 particles were identified on the surface using electron microprobe analysis. Quantitative analysis from randomly selected spots on the surface showed a large variation in the amount of copper present from a high of 27.6 percent to a low of 6.1 percent. No pattern of Cu content versus surface position or surface features was found.

X-ray spectroscopy analysis shows the Cu concentration in this sample as a whole to be 23.2 percent. This analysis, of course, is representative more of the surface of the sample than of the interior.

Emission spectrographic analysis of some of the material from the center of the specimen gave the following trace elemental content:

Si - 20 PPM

Fe - 20 PPM

Ag - 20 PPM

Pb - 5 PPM

Ca - 6 PPM

Electron microprobe analysis from selected areas on the specimen cross section showed the copper concentration near the flat side and in the center to be almost equal and averaged 28.4 percent. In the region near the cap, however, the average dropped to 25.6 percent.

Figure 13 is an optical macrograph of the polished and etched cross section of Specimen SL-1.8. Optical and scanning electron micrographs of the microstructures are shown in Figures 14 through 20. Figure 14 shows the microstructure in the cap region of the specimen. The porosity and microstructure associated with the external porous band are shown in Figures 15 and 16. The random equiaxed dendrites in the center of the section are shown in Figures 17 and 18 and the columnar dendrites near the flat region are shown in Figures 19 and 20.

Specimen SL-1.7

Specimen SL-1.7 is a nickel-copper alloy and resembles Specimen SL-1.8 very closely as seen in Figure 21. It has a smooth flat side and the three regions of surface topography previously described for Specimen SL-1.8.

The density of Specimen SL-1.7 was measured to be 8.97×10^{-6} kg/m^3.

The sphericity was found to be 1.08 (Rmax/Rmin).

The Laue grain size was measured to be somewhat greater than 1×10^{-5}m. The surface grain size was measured in the cap area and in the porous area of free dendrites. In the cap area the dendrites measured 6.7×10^{-5}m and in the free dendrite area they measured 7×10^{-5}m($\pm 5 \times 10^{-5}$m).

Figure 22 is a scanning electron micrograph of the surface of Specimen SL-1.7 in the columnar dendritic region. The structure in the more porous band is shown in Figure 23 and the boundary region between the porous band and the cap area is shown in Figure 24. Figures 25 and 26 show the surface structure of the cap area.

Energy dispersive analyses of a number of areas on the surface of the specimen showed the following contaminating elements:

Al, W, Ag, Sn, Fe, and Cr

The copper content in the cap area was analyzed in the electron microprobe. An overall analysis in the area gave the copper content to be 9.05 percent. Point analyses along these surface dendrites showed a variation according to the growth pattern from a high of 11.53 percent to a low of 7.82 percent.

Microprobe analyses from areas on the cross section of this specimen showed a general decrease in the amount of copper present in dendrites as analysis proceeded from the flat region toward the cap region. The average copper content in dendrites in areas other than the cap region was 25.4 percent. In interdendritic points it averaged 42.3 percent. In or near the cap area the copper content in the dendrites measured to be 22.5 percent and in interdendritic spots it was 41.2 percent. Quantitative analyses were also made in the electron microprobe along radii of the cross section in both the central dendritic portion and in the cap area of the specimen. Figure 27 is a graph of the copper concentration versus distance from the specimen surface in the central dendritic region. The minimas on this graph represent

the center of the dendritic arm sections as presented on the specimen cross section and are not necessarily the minimum copper content of the true center of a dendritic arm. Figure 28 is a graph of copper content versus distance from the surface in the cap region of the specimen. Note the low copper concentration at the surface of these dendrites.

The lattice parameter was measured using the cross section and found to be 3.5500×10^{-10} m.

The Curie Point was measured for both the bulk sample and for the surface depletion region. It was found for the bulk sample to be less than 77°K and for surface depletion region to be around 520°K.

Figure 29 is an optical micrograph of the polished and etched section showing the microstructure in the boundary region between the porous band and the cap area. Internal dendritic grain size measurements were made in the columnar grain area and in the free dendritic regions. In the columnar region the dendrites averaged 4×10^{-3} m long and 1.4×10^{-3}m wide. In the free dendrite region they averaged 0.44×10^{-3} m in diameter.

DISCUSSION OF RESULTS

The internal microstructures and external appearances of the nickel-copper alloy specimens processed in near zero gravity are very similar to those found on the ground test specimens of the same alloy. The three surface textures, the smooth columnar dendrites, the equiaxed dendrites in a porous band, and the continuous cap of fine circular dendrites, are present in specimens from both experiments and comprise approximately the same areas in all specimens. The columnar dendrites grew in all cases as a result of the temperature gradient created by the contact of the specimens with some other surface. None of the specimens solidified in free flight. In the microstructures seen in the cross sections of these specimens the columnar dendrites appear slightly larger in the near zero gravity specimens than they do in the ground base specimens. As solidification continued the temperature gradient lessened and the columnar dendritic growth gave way to the growth of the randomly oriented equiaxed dendrites. The porosity seen on the surfaces of the specimens in the area of these equiaxed dendrites is due to solidification shrinkage. At some time before final solidification of the specimen the cap area of "two-dimensional" circular dendrites was formed. This area is free of porosity and is typical of chilled surfaces formed on castings.

There is evidence that more copper was lost by evaporation in the specimens processed in near zero gravity conditions but this is clouded by the fact that the ground base specimens contained unmelted portions.

The microsegregation in the dendritic and interdendritic regions is not unusual and is in agreement with the phase diagram for this alloy. No large voids were found in the interior of any of these specimens.

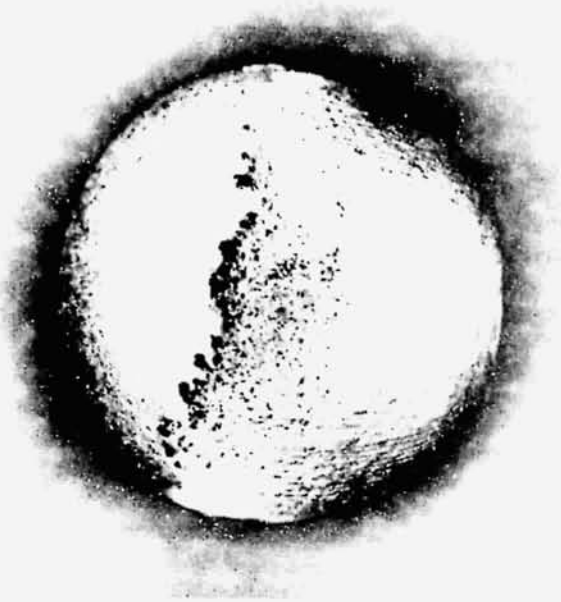

Georgia Tech
Figure 1. Profile view of Specimen SL-1.8 (10X).

Georgia Tech
Figure 2. Profile view of ground base Specimen 2-10 (10X).

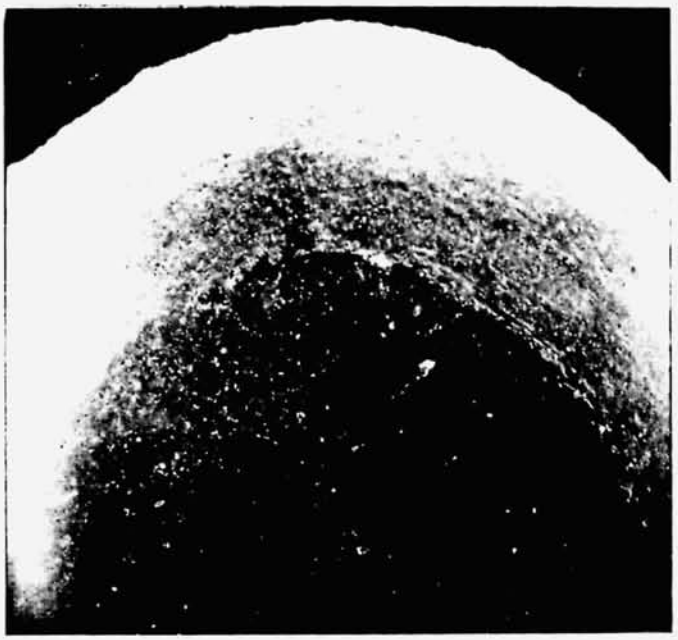

Georgia Tech

Figure 3. Scanning electron micrograph taken normal to flat area on Specimen SL-1.8 (25X).

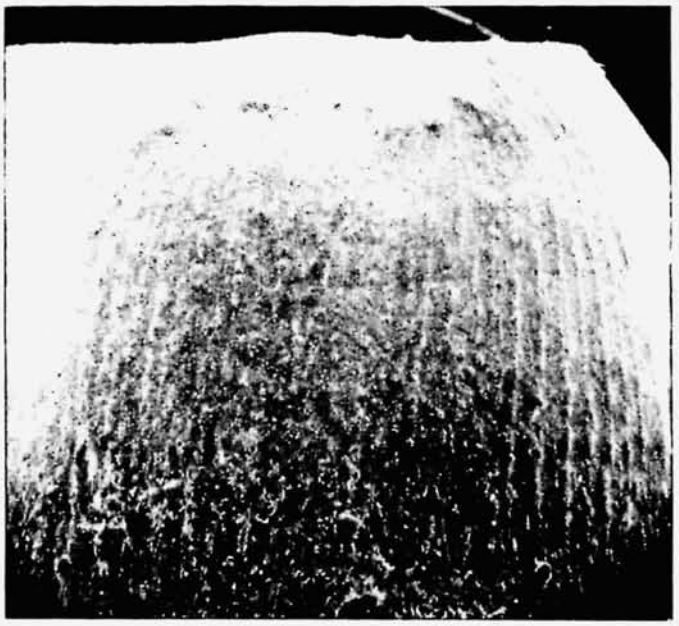

Georgia Tech

Figure 4. Scanning electron micrograph of columnar dendrites on the surface of Specimen SL-1.8 (25X).

Georgia Tech

Figure 5. Scanning electron micrograph of columnar dendrites on the surface of Specimen SL-1.8 (250X).

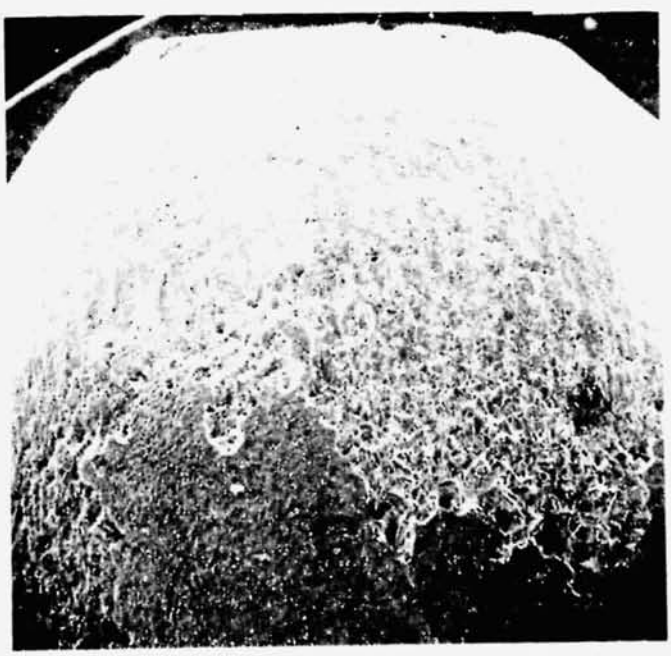

Georgia Tech

Figure 6. Scanning electron micrograph showing the three surface textures on Specimen SL-1.8 (25X).

Georgia Tech

Figure 7. Scanning electron micrograph of the abrupt transition from the porous band to the cap area in Specimen SL-1.8 (250X).

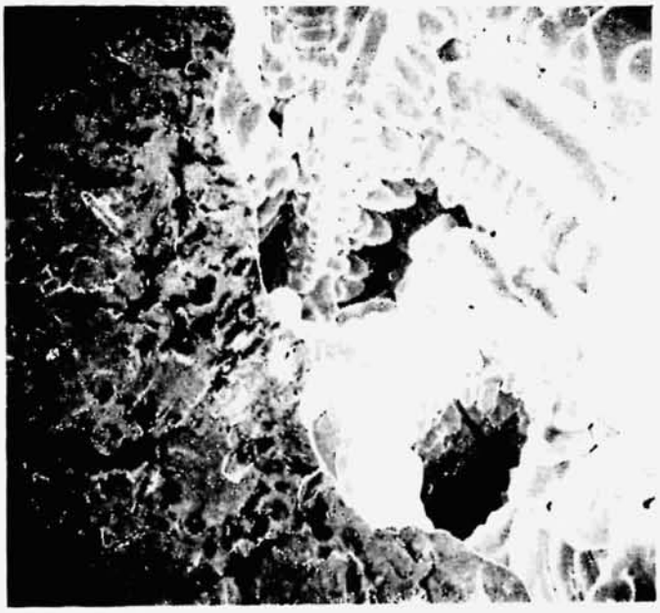

Georgia Tech

Figure 8. Scanning electron micrograph of the abrupt transition from the porous band to the cap area in Specimen SL-1.8 (250X).

Georgia Tech

Figure 9. Scanning electron micrograph of the circular dendrites in the cap region of Specimen SL-1.8 (250X).

Georgia Tech

Figure 10. Scanning electron micrograph of the circular dendrites in the cap region of Specimen SL-1.8 (250X).

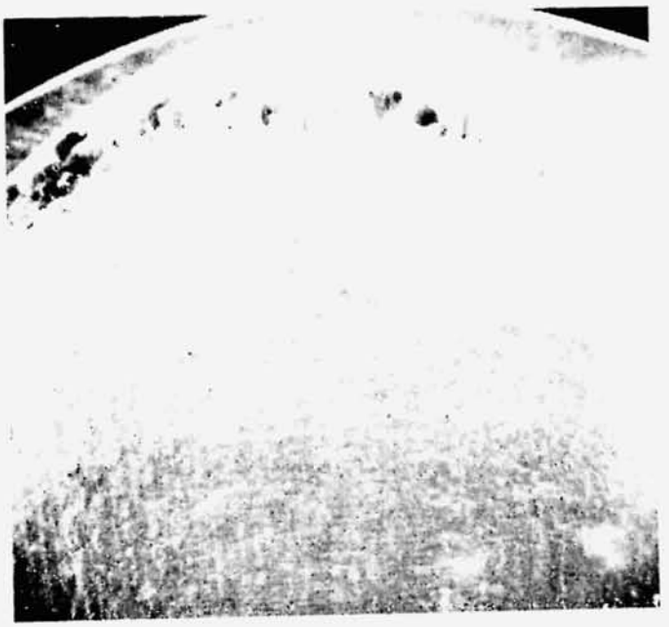

Georgia Tech

Figure 11. Oblique view of the cap boundary on Specimen SL-1, S (25X).

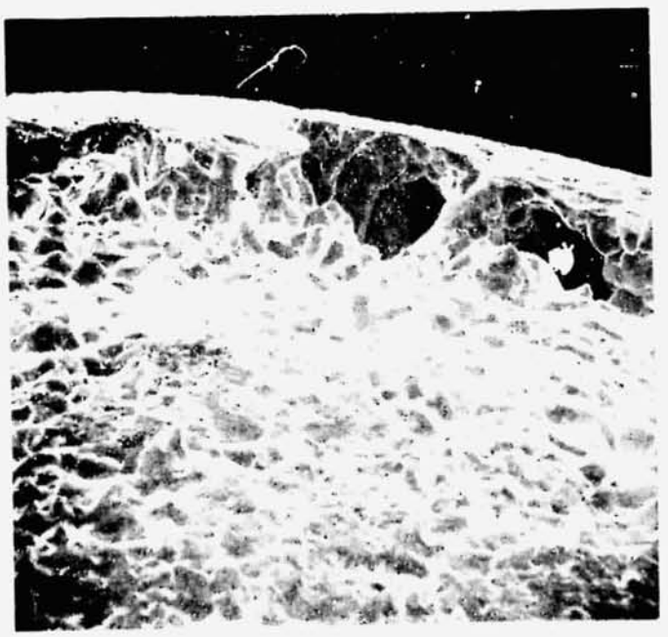

Georgia Tech

Figure 12. Oblique view of the cap boundary on Specimen SL-1, S (100X).

Georgia Tech

Figure 13. Optical macrograph of the polished and etched cross section of Specimen SL-1.8 (10X).

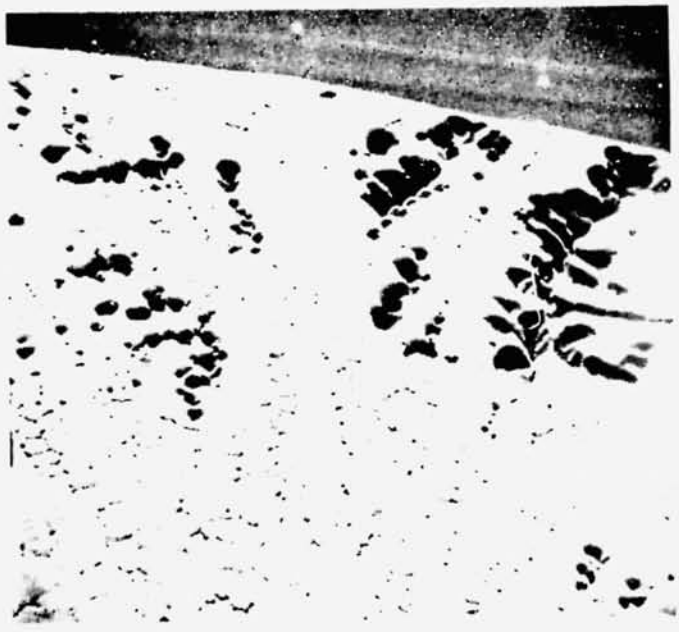

Georgia Tech

Figure 14. Scanning electron micrograph of the cross section of Specimen SL-1.8 near the cap region (100X).

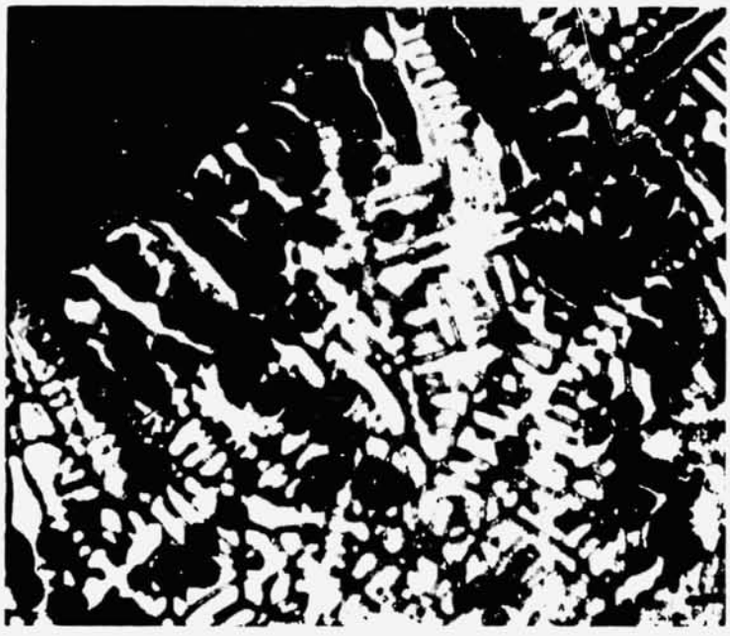

Georgia Tech

Figure 15. Optical micrograph of the cross section of Specimen SL-1.8 near the porous band (100X).

Georgia Tech

Figure 16. Scanning electron micrograph of the cross section of Specimen SL-1.8 near the porous band (100X).

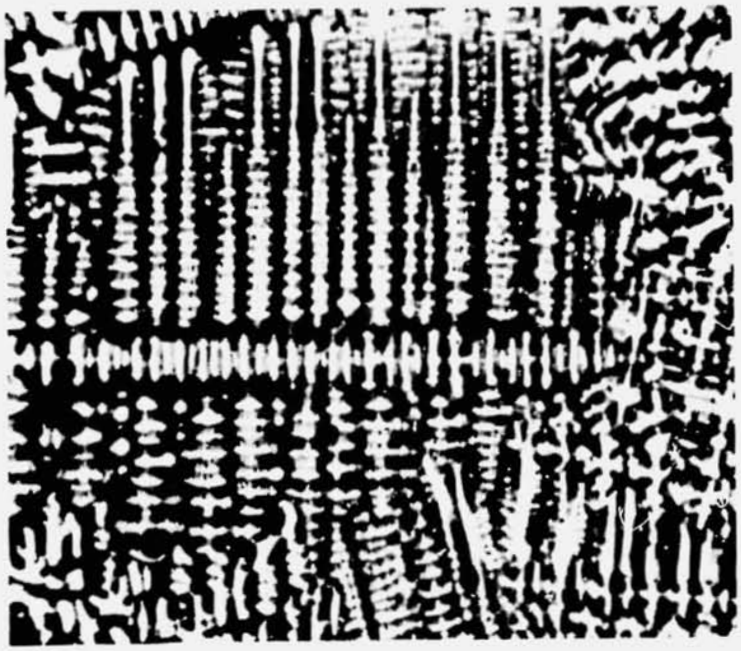

Georgia Tech

Figure 17. Optical micrograph of the cross section of Specimen SL-1.8 in the equiaxed dendritic region (100X).

Georgia Tech

Figure 18. Scanning electron micrograph of the cross section of Specimen SL-1.8 in the equiaxed dendritic region (250X).

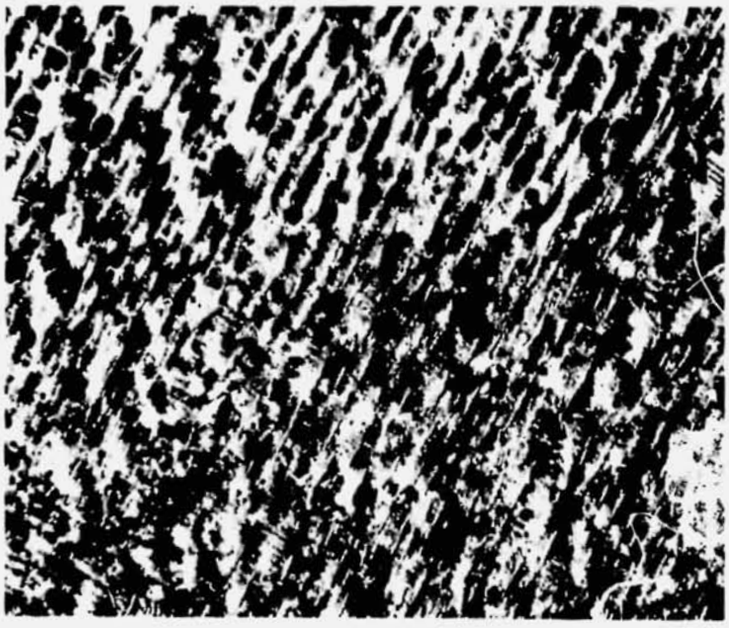

Georgia Tech

Figure 19. Optical micrograph of the columnar dendrites in the cross section of Specimen SL-1.8 (100X).

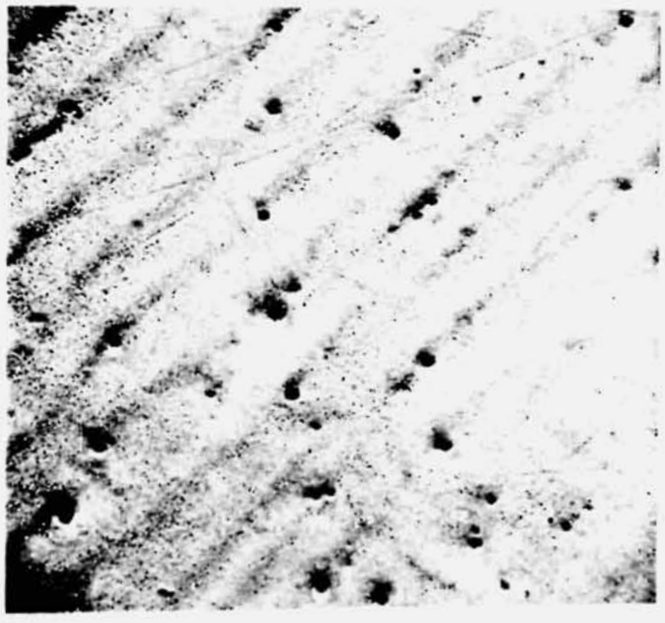

Georgia Tech

Figure 20. Scanning electron micrograph of the columnar dendrites in the cross section of Specimen SL-1.8 (100X).

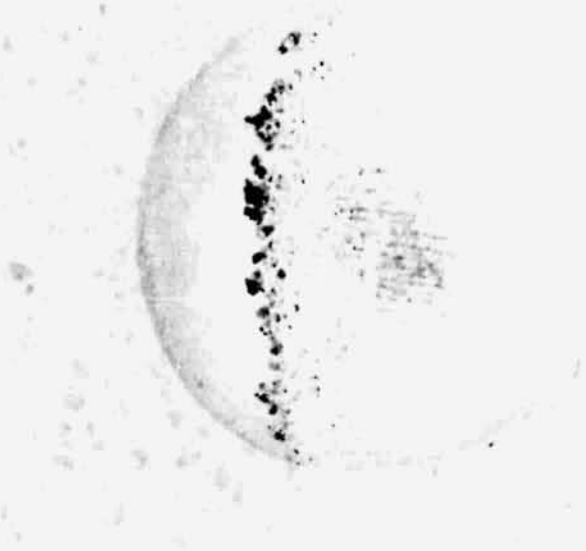

Grumman Aerospace

Figure 21. Profile view of Specimen SL-1.7 (10X).

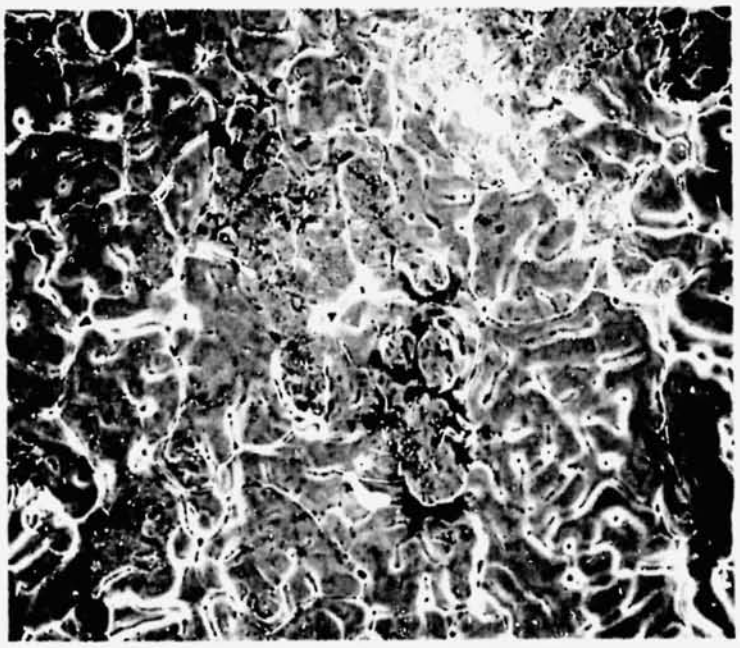

Grumman Aerospace

Figure 22. Scanning electron micrograph of columnar dendrites on the surface of Specimen SL-1.7 (400X).

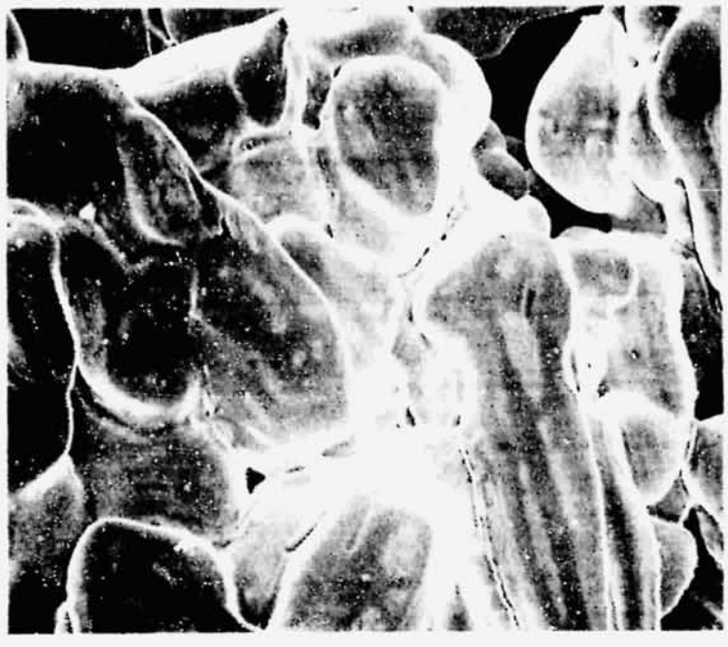

Grumman Aerospace

Figure 23. Scanning electron micrograph of the dendrites in the porous band on Specimen SL-1.7 (750X).

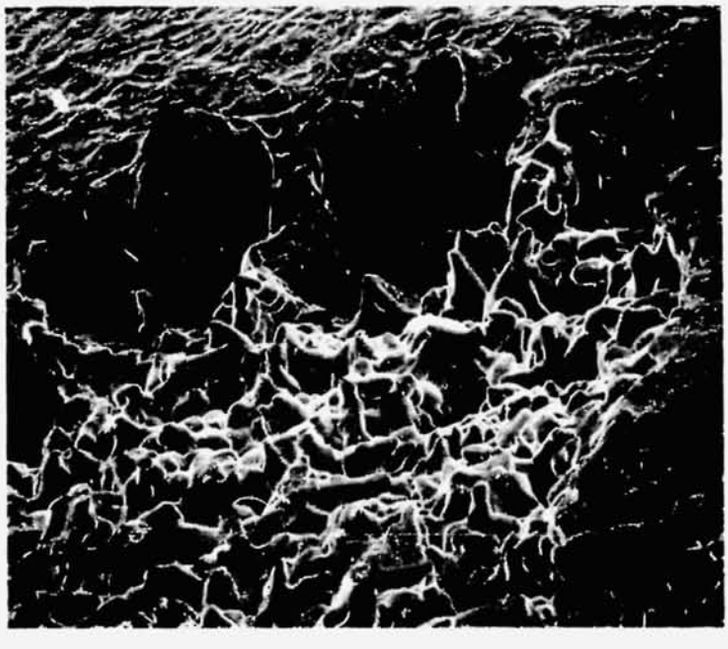

Grumman Aerospace

Figure 24. Scanning electron micrograph of the edge of the cap region on Specimen SL-1.7 (150X).

Grumman Aerospace

Figure 25. Scanning electron micrograph of the circular dendrites in the cap region of Specimen SL-1.7 (750X).

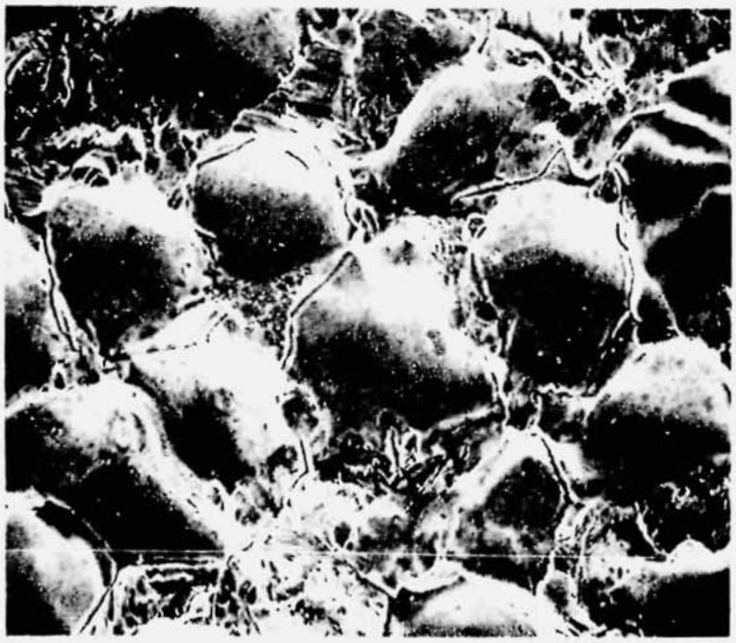

Grumman Aerospace

Figure 26. Scanning electron micrograph of the circular dendrites in the cap region of Specimen SL-1.7 (750X).

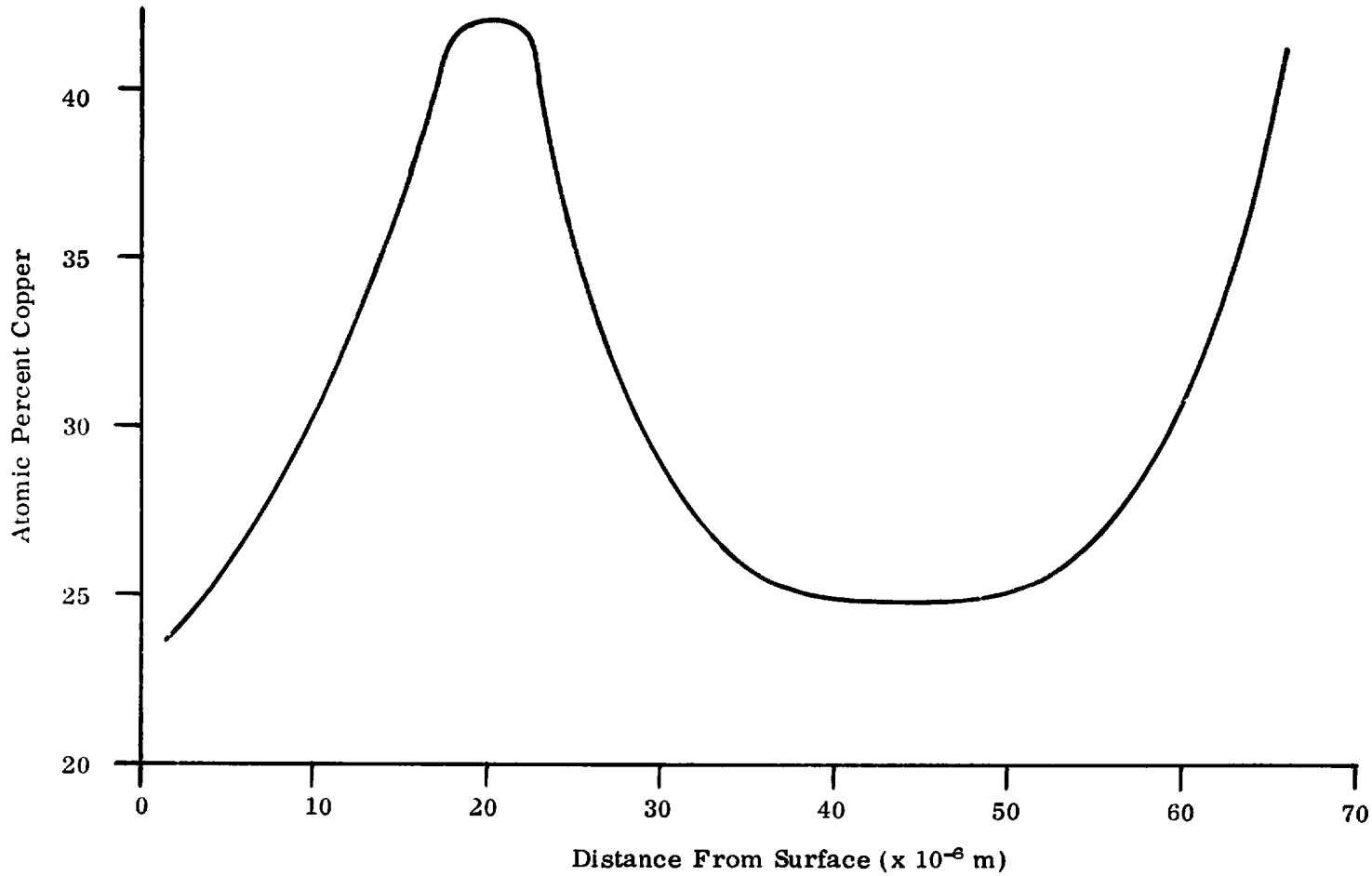

Figure 27. Copper concentration versus distance from specimen surface in the central dendritic region of Specimen SL-1.7.

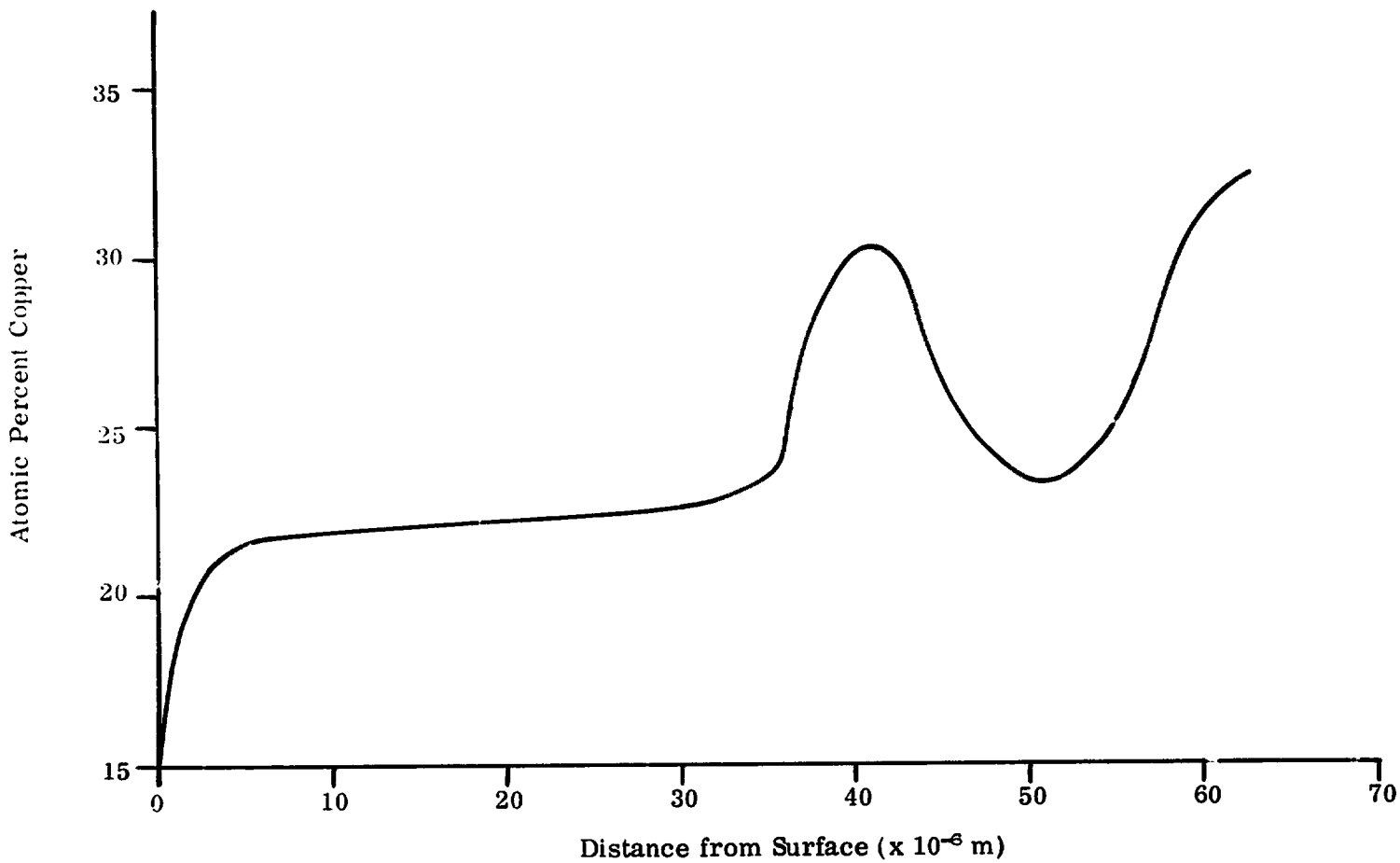

Figure 28. Copper concentration versus distance from specimen surface in the cap region of Specimen SL-1.7.

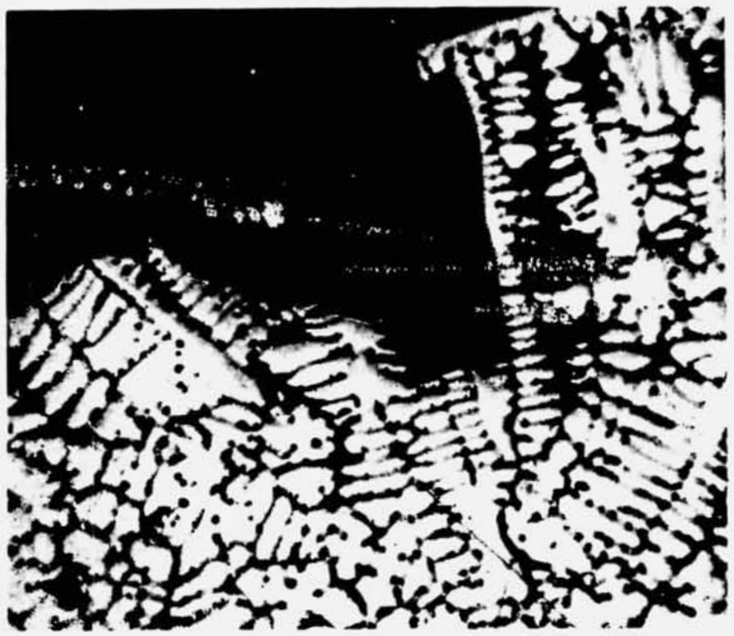

Grumman Aerospace

Figure 29. Optical micrograph of the polished and etched cross section of Specimen SL-1.7 at the edge of the cap area (100X).